Macular Atrophy in Birdshot Retinochoroidopathy: An Optical Coherence Tomography and Multifocal Electroretinography Analysis

David G. Birch[1,2], **Patrick D. Williams**[2,3], **David Callanan**[2,3], **Robert Wang**[2,3], **Kirsten G. Locke**[1], and **Donald C. Hood**[4]

[1] The Retina Foundation of the Southwest, Dallas, TX

[2] University of Texas Southwestern Medical Center, Dallas, TX

[3] Texas Retina Associates, Arlington, TX

[4] Departments of Psychology and Ophthalmology, Columbia University, New York, NY

Introduction

Birdshot retinochoroidopathy is an uncommon intraocular inflammatory disorder (uveitis) comprised of depigmented spots in the choroid along with vitreous cells [1,2]. Anterior inflammation may be present, and the disease is typically bilateral and symmetric. Retinal capillary hyperpermeability and resultant cystoid macular edema are common [3].

Some reports have suggested stability of visual acuity after an initial inflammatory stage [4, 5]. Others, however, have described a chronic and unrelenting course [1,2,6–8]. Serial electroretinograms and visual fields support progressive deterioration of retinal function, even in cases not considered to have active inflammation [6,8]. Although retinal atrophy has been mentioned in birdshot retinochoroidopathy [6,7], there is only one case report specifically describing macular atrophy [9]. Autofluorescence imaging has demonstrated the extent of retinal pigment epithelium (RPE) atrophy, even in regions without hypopigmented birdshot lesions [10]. Histopathology has been performed in birdshot retinochoroidopathy, but without mention of retinal thickness away from the fovea or retinal atrophy [11].

Optical coherence tomography (OCT) of birdshot retinochoroidopathy has revealed features of the choroidal lesions [9,12]. OCT and retinal thickness analysis were used to evaluate systemic steroid treatment in birdshot retinochoroidopathy in a case report, but retinal thickness was normal away from the fovea [12].

Recent advances in electroretinography and optical imaging allow for more detailed analysis of the macula than previously possible. The multifocal (mf) ERG produces a detailed topographical map of retinal function, while frequency domain (fd) OCT provides a precise analysis of layer-by-layer structure within the macula. The purpose of this study is to evaluate macular atrophy by fdOCT in patients with birdshot retinochoroidopathy and to compare the resulting thickness measures with visual acuity and mfERG.

Corresponding author: David G. Birch, Retina Foundation of the Southwest, 9900 North Central Expressway, Dallas, TX 75231 phone: 214-363-3911, dbirch@retinafoundation.org.

Methods

Seven patients with previous OCT-3 (Zeiss Stratus OCT-3) consented to participate in this study after all procedures were explained. Inclusion criteria included a diagnosis of birdshot retinochoroidopathy, a positive HLA-A29 serotype, myopia < 5.00 diopters, and clear ocular media. The clinical charts of these patients were reviewed for demographic information, length of time with a diagnosis of birdshot retinochoroidopathy, previous treatments, and ocular history. Macular thinning was defined from the OCT-3 as a foveal thickness less than 160 μm and a macular volume less than 6 mm^3.

Following informed consent, mfERGs were obtained with the Veris Science 5.1 system using the fundus camera display system [13] and followed ISCEV guidelines [14]. The stimulus configuration consisted of 103 hexagonal elements scaled for retinal eccentricity and modulated in luminance according to a pre-determined pseudo-random sequence. The maximum luminance of the display was 200 cd/m^2 and the minimum was 2 cd/m^2. All responses were measured as trough to peak amplitude density (nV/deg2). Normal values were derived from 20 volunteers ages 21–65 years with normal visual acuity and normal eye exams.

To determine which layers of the retina were primarily responsible for macular thinning, each patient was asked to return for fdOCT (Spectralis HRA+OCT; Heidelberg Engineering, Heidelberg, Germany). The confocal scanning laser ophthalmoscope (cSLO) system provides infrared reflectance(IR; 820 nm) imaging. Optical resolution is approximately 10 μm. The fdOCT runs simultaneously with the cSLO imaging system, using a second, independent pair of scanning mirrors. The wavelength of the fdOCT imaging system is 870 nm. Optical resolution is approximately 7 μm in depth and 14 μm transversely. The scans included at least one 9 mm horizontal scan through the midline and peripapillary scans using the 3.4 mm circle scan of the fdOCT. Results from the seven patients were compared to segmented data from 23 normals [15].

Segmentation of retinal layers was done by hand with software included with the Spectralis system. The operator measured the thickness of each retinal layer at 6 locations along the horizontal midline (fovea, 3° and 9° nasal retina, 3°, 9° and 15° temporal retina). Five boundaries, labeled A through E in Fig. 1, were identified and labeled. These were chosen because there appears to be general consensus on their identification [16–19].

A. Vitreous/RNFL: the inner limiting membrane (i.e. the boundary between the vitreous and the RNFL).

B. RFNL/GCL: the boundary between the RFNL and the ganglion cell layer (GCL).

C. IPL/INL: the boundary between the inner plexiform layer (IPL) and the inner nuclear layer (INL).

D. INL/OPL: the border between the INL and the outer plexiform layer (OPL).

E. BM/choroid: the boundary between Bruch's membrane (BM) and the choroid.

Using the locations of these boundaries, we defined 4 retinal regions/layers for comparing patients to controls:

1. Total Retinal thickness (Total) is the distance between A and E.

2. Retinal nerve fiber layer thickness (RFNL) is the distance between A and B.

3. Inner nuclear layer thickness (INL) is the distance between C and D.

4. Outer plexiform layer, photoreceptor and RPE thickness (REC+) is the distance between D and E.

Statistical comparisons (t-tests and Pearson r) were performed with Statistica version 7.1 (StatSoft, Tulsa OK). All procedures relating to human subjects conformed to the Declaration of Helsinki and were approved by the Institutional review board of UT Southwestern Medical Center.

Results

Demographic data are presented in Table 1. The duration since the initial diagnosis of birdshot chorioretinopathy ranged from 2 to 16 years. Previous treatments for vitritis and cystoid macular edema included periocular and intraocular triamcinolone as well as oral azathioprine, mycophenolate, acetazolamide, and prednisone. Four eyes were treated with flucinolone implants (Retisert™, Bausch & Lomb, St. Louis, MO). Of these, three developed secondary glaucoma, and two required tube-shunt placement. No eyes had appreciable iritis or vitritis during the time of examination. Also, no optic nerve pallor was documented in any eyes. All eyes exhibited typical choroidal birdshot lesions.

As shown in Table 2, eyes were separated based on the presence of anatomic thinning on OCT-3. Visual acuities are shown with the results of electrophysiologic testing in Table 3. Eyes with anatomic thinning are highlighted in bold. All eyes with history of birdshot for greater than 10 years, including those without anatomic thinning, had below average mfERG results based on both the fovea and on the mean response density derived from all six rings.

Mean Snellen acuity, mean foveal thickness, mean macular volume, mean foveal ERG response density and mean overall mfERG response density of eyes (n= 6) with anatomic thinning on OCT-3 were compared to the values for eyes (n = 8) without anatomic thinning (Table 4). There was a significance difference ($p < 0.01$) between eyes with anatomic thinning and eyes without anatomic thinning on all measures. Across all eyes, there were significant correlations between foveal ERG response density and logMAR visual acuity ($r = -0.71$, $p < 0.05$) and between OCT-3 foveal thickness and both logMAR visual acuity ($r = -0.76$, $p < 0.05$) and foveal ERG response density ($r = 0.62$, $p < 0.05$). The duration since initial diagnosis was correlated with both foveal ERG response density ($r = -0.67$, $p < 0.05$) and mean mfERG response density ($r = -0.55$, $p < 0.05$).

Left eye fdOCT midline scans from a normal subject and patient #1 are shown in Figure 1. Segmentation lines are added to highlight optical boundaries that were used to distinguish retinal layers. Right eye fdOCT midline scans of all seven patients are shown in Figure 2. Also shown are mfERG responses and 3-dimensional plots from the central 40 degrees. Clearly, there is a qualitative correspondence between the mfERG and fdOCT data. Patients #1 and #3 showed thinning of the photoreceptor layer across the midline and borderline detectable mfERGs. The small mfERG from the fovea in patient #3 corresponds to the approximately 500 micron diameter patch of preserved photoreceptors in the fovea. Patients #4 and #6 had the thickest receptor layers and almost normal mfERG patterns. Patients #2, #5 and #7 were intermediate, with patchy areas of photoreceptor thinning and regional loss of mfERG responses. Note that #7 has abnormal mfERG timing from the fovea, presumably related to what appears to be a foveal neurosensory detachment.

To determine whether the RFNL was of normal thickness in these patients, peripapillary scans were obtained from all eyes with the fdOCT 3.4 mm circular scan. With the exception of patient #1, all eyes had normal peripapillary scans. Patient #1 was below machine normal limits in the superior-nasal and inferior-nasal quadrants of both eyes, consistent with reduced numbers of arcuate nerve fibers. RNFL thickness was also measured from scans along the horizontal meridian (Figure 1) at a location 2.5 nasal to the fovea. For the 23 normal subjects, the mean RNFL thichness at this location was 45.1 mm (95% confidence interval = 30.9 – 59.3 mm).

For the patients with birdshot chorioretinopathy, 8 of 14 had RNFL thickness within the normal range, while 6 of 14 had RNFL thickness slightly greater than normal.

Total retinal thickness (Total), outer plexiform layer, photoreceptor and RPE thickness (Rec +) and inner nuclear layer thickness are shown for measures from the horizontal meridian in all 14 eyes from the 7 patients in Figure 3. Mean thickness for 23 normal subjects is shown as the bold curve in each plot; ± 2 standard deviations are shown as the shaded area. For total retinal thickness (top), all eyes were below mean normal in thickness at all locations and many were reduced by greater than 2 standard deviations. As shown in the middle plot, the reduction in retinal thickness was associated with a reduction in Rec+, the segment extending from the proximal border of the outer plexiform layer to the Bruch's membrane/choroid interface. This segment thus reflects photoreceptor cells and RPE. The inner retinal layer thickness (bottom plot) was within normal limits at most eccentricities in most patients; the exceptions were in the regions of cystic swelling in patients #1, and #2.

Discussion

Based on the results of this study, anatomic macular thinning is associated with severe vision loss in patients with birdshot retinochoroidopathy. All patients with atrophy had an extensive history of birdshot retinochoroidopathy with the minimum time from diagnosis being ten years. Macular and chorioretinal atrophy in longstanding birdshot retinochoroidopathy has been mentioned in the literature, although without specific evaluation [6,7,9]. In these reports, permanent vision loss is well described. The present study corroborates the long-term visual prognosis in patients with birdshot retinochoroidopathy and provides further evidence that the decline is due to progressive deterioration of the photoreceptors, RPE, and choroid.

Optic atrophy could, hypothetically, account for retinal thinning with loss of the ganglion cell layer and nerve fiber layer. Optic atrophy has been described in birdshot retinochoroidopathy [20,21]. However, none of the patients in the present study had any optic pallor. Peripapillary RNFL scans were normal in all but one patient, and RNFL thickness measured adjacent to the optic disk was within normal limits or slightly greater than normal in all eyes.

The fdOCT measures provide direct evidence that the major cause of macular thinning in birdshot is thinning of the outer retina. As shown in Figure 3, most patients showed normal inner nuclear layer thickness. The two exceptions were patients 1 and 2, both of whom had macula edema. Virtually all patients, however, showed significant thinning in the extended photoreceptor component (Rec+), which included the outer plexiform layer, the photoreceptor nuclei, inner and outer segments and the RPE. The only exception was the right eye of patient 7, where a neurosensory retinal detachment in the fovea complicated the measure of REC+.

The exact etiology of the macular thinning is unknown, although it suggests retinal cell death, either by direct or indirect means. A possible confounding effect is the association of outer retinal atrophy with long-term steroid use [22,23]. Given the limited exposure in these patients, however, macular thinning is more likely to be due to retinal autoimmunity specific to birdshot retinochoroidopathy. Although the striking clinical features of birdshot retinochoroidopathy are the choroidal lesions, retinal S-antigen has been found as a potential basis for autoimmunity [24]. Alternatively, non-specific chronic inflammation may induce apoptosis within the retina and choroid, leading to eventual structural atrophy and functional decline [25].

Asymmetric retinal degeneration was observed in this study. Two of the seven patients had unilateral retinal thinning (patients 2 and 5) and two had bilateral thinning (patients 1 and 3). For patient 2, visual acuity in the unaffected eye was only one line better than the affected eye. For patient 5, the eye with thinning had much poorer acuity than the eye without thinning. Patients 1 and 2 had some retinal thickening temporal to the fovea, demonstrating the possibility

of diffuse macular atrophy and concomitant intraretinal cysts. This intraretinal swelling may have confounded functional examinations as well.

In addition to structural changes seen on fdOCT, there were also functional changes. The mfERGs were significantly altered in most eyes with macular atrophy. The correlation of mfERG results with OCT findings and visual acuity was clearly evident in patients with severe anatomic atrophy, but was less consistent in patients with mild changes in vision, OCT, or ERG. Even in patients without anatomic thinning, the mfERG results were below average. A longitudinal study would be required to assess the predictive value of mfERG in birdshot patients. A decline in mfERG may precede severe acuity decline and assist the clinician in deciding which patients require additional treatment.

Earlier reports of full-field electroretinography of eyes with birdshot retinochoroidopathy have demonstrated an initial decreased amplitude and increased latency of the b-wave as well as loss of oscillatory potentials, suggesting dysfunction of the inner retina [6,26]. As the disease progressed, the electroretinographic dysfunction became evident in both the inner and outer retina. Loss of visual acuity appeared to lag behind electroretinographic dysfunction. This phenomenon might explain the preservation of visual acuity in some of the eyes in this study.

The results of this study suggest that both fdOCT and mfERG may serve as useful adjuncts in the evaluation of birdshot retinochoroidopathy, not only to assess macular edema but also to assess retinal atrophy and early decline. Further study is required to detail the true etiology of retinal atrophy on OCT in patients with birdshot retinochoroidopathy, whether OCT or mfERG has prognostic value in these patients, and whether treatment of associated uveitis may prevent eventual retinal atrophy.

Acknowledgments

References

1. Ryan SJ, Maumenee AE. Birdshot retinochoroidopathy. Am J Ophthalmol 1980;89:31–45. [PubMed: 7356785]

2. Kaplan HJ, Aaberg TM. Birdshot retinochoroidopathy. Am J Ophthalmol 1980;90:773–782. [PubMed: 7446664]

3. Thorne JE, et al. Birdshot retinochoroidopathy: ocular complications and visual impairment. Am J Ophthalmol 2005;140:45–51. [PubMed: 16038650]

4. Preim HA, Oosterhuis JA. Birdshot chorioretinopathy: Clinical characteristics and evolution. Br J Ophthalmol 1988;72:646–659. [PubMed: 2460128]

5. Gass JD. Vitiliginous chorioretinitis. Arch Ophthalmol 1981:1778–1787. [PubMed: 7295126]

6. Oh KT, Christmas NJ, Folk JC. Birdshot retinochoroiditis: Long term follow-up of a chronically progressive disease. Am J Ophthalmol 2002;133:622–629. [PubMed: 11992859]

7. Rothova A, et al. Birdshot chorioretinopathy: long-term manifestations and visual prognosis. Ophthalmology 2004;111:954–9. [PubMed: 15121374]

8. Thorne JE, et al. Loss of visual field among patients with birdshot chorioretinopathy. Amer J Ophthalmol 2008;145:23–28. [PubMed: 17997394]

9. Witkin AJ, et al. Ultrahigh resolution optical coherence tomography of birdshot retinochoroidopathy. Br J Ophthalmol 2005;89:1660–1671. [PubMed: 16299151]

10. Koizumi H, Pozzoni MC, Spaide RF. Fundus autofluorescence in birdshot chorioretinopathy. Ophthalmology 2008;115:15–20.

11. Gaudio PA, Kaye DB, Crawford JB. Histopathology of birdshot retinochoroidopathy. Br J Ophthalmol 2002;86:1439–41. [PubMed: 12446382]

12. De Geronimo F, et al. Birdshot retinochoroidopathy: measurement of the posterior fundus spots and macular edema using a retinal thickness analyzer, before and after treatment. Eur J Ophthalmol 2000;10:338–40. [PubMed: 11192845]

13. Birch, DG. Focal and multifocal electroretinography. In: Fishman, GA., et al., editors. Electrophysiologic Testing. American Academy of Ophthalmology; San Francisco: 2001. p. 177-195.

14. Hood DC, et al. ISCEV guidelines for clinical multifocal electroretinography (2007 edition). Doc Ophthalmol 2008;116(1):1–11. [PubMed: 17972125]

15. Hood DC, et al. Thickness of receptor and post-receptor retinal layers in patients with retinitis pigmentosa measured with frequency-domain optical coherence tomography (fdOCT). Invest Ophthalmol Vis Sci. 2008 Epub ahead of print.

16. Srinivasan V, et al. Characterization of outer retinal morphology with high-speed, ultrahigh-resolution optical coherence tomography. Invest Ophthalmol Vis Sci 2008;49(4):1571–1579. [PubMed: 18385077]

17. Chen T, et al. Spectral Domain Optical Coherence Tomography: ultra-high speed, ultra-high resolution ophthalmic imaging. Arch Ophthalmol 2005;123:1715–1720. [PubMed: 16344444]

18. Drexler W, Fujimoto JG. State-of-the-art retinal optical coherence tomography. Prog Retin Eye Res 2008;27(1):45–88. [PubMed: 18036865]

19. Witkin AJ, et al. Ultra-high resolution optical coherence tomography assessment of photoreceptors in retinitis pigmentosa and related diseases. Am J Ophthalmol 2006;142(6):945–52. [PubMed: 17157580]

20. Willermain F, Greiner K, Forrester JV. Atypical end-stage birdshot retinochoroidopathy. Ocul Immunol Inflamm 2003;11:305–307. [PubMed: 14704902]

21. Caballero-Presencia A, Diaz-Guia E, Lopez-Lopez JM. Acute anterior ischemic optic neuropathy in birdshot retinochoroidopathy. Ophthalmologica 1988;196:87–91. [PubMed: 3362511]

22. Loo JL, Lee SY, Ang CL. Can long-term corticosteroids lead to blindness? A case series of central serous chorioretinopathy induced by corticosteroids. Annals Academy of Medicine 2006;35:497–499.

23. Tittl MK, et al. Systemic findings associated with central serous chorioretinopathy. Amer J Ophthalmol 1999;12(81):63–68. [PubMed: 10482095]

24. Nussenblatt RB, et al. Birdshot retinochoroidopathy associated with HLA-A29 antigen and immune responsiveness to retinal S-antigen. Am J Ophthalmol 1982;94:147–158. [PubMed: 6956239]

25. Chan CC, et al. Apoptosis in patients with posterior uveitis. Arch Ophthalmol 1997;115:1559–1567. [PubMed: 9400790]

26. Zacks DN, et al. Electroretinograms as an indicator of disease activity in birdshot retinochoroidopathy. Graefes Arch Clin Exp Ophthalmol 2002:601–607. [PubMed: 12192452]
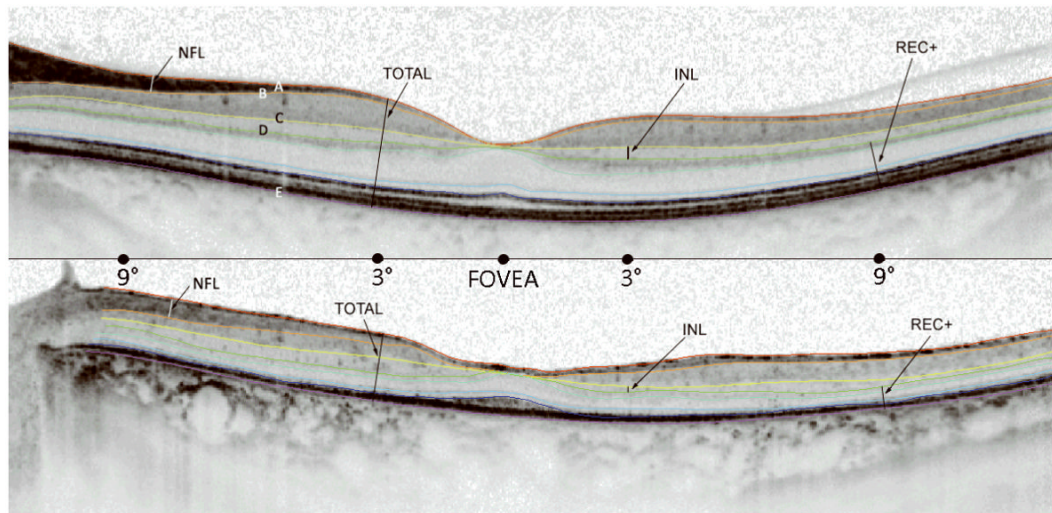
Figure 1.
Segmentation of fdOCT horizontal midline scans in a normal subject (top) and patient #1 with birdshot retinochoroidopathy (bottom). A. Vitreous/RNFL B. RFNL/GCL C. IPL/INL D. INL/ OPL E. BM/choroid. Total Retinal Thickness (TR) is the distance between A and E. Retinal nerve fiber layer thickness (RNFL) is the distance between A and B. Inner nuclear layer thickness (INL) is the distance between C and D. REC+ is the distance between D and E.
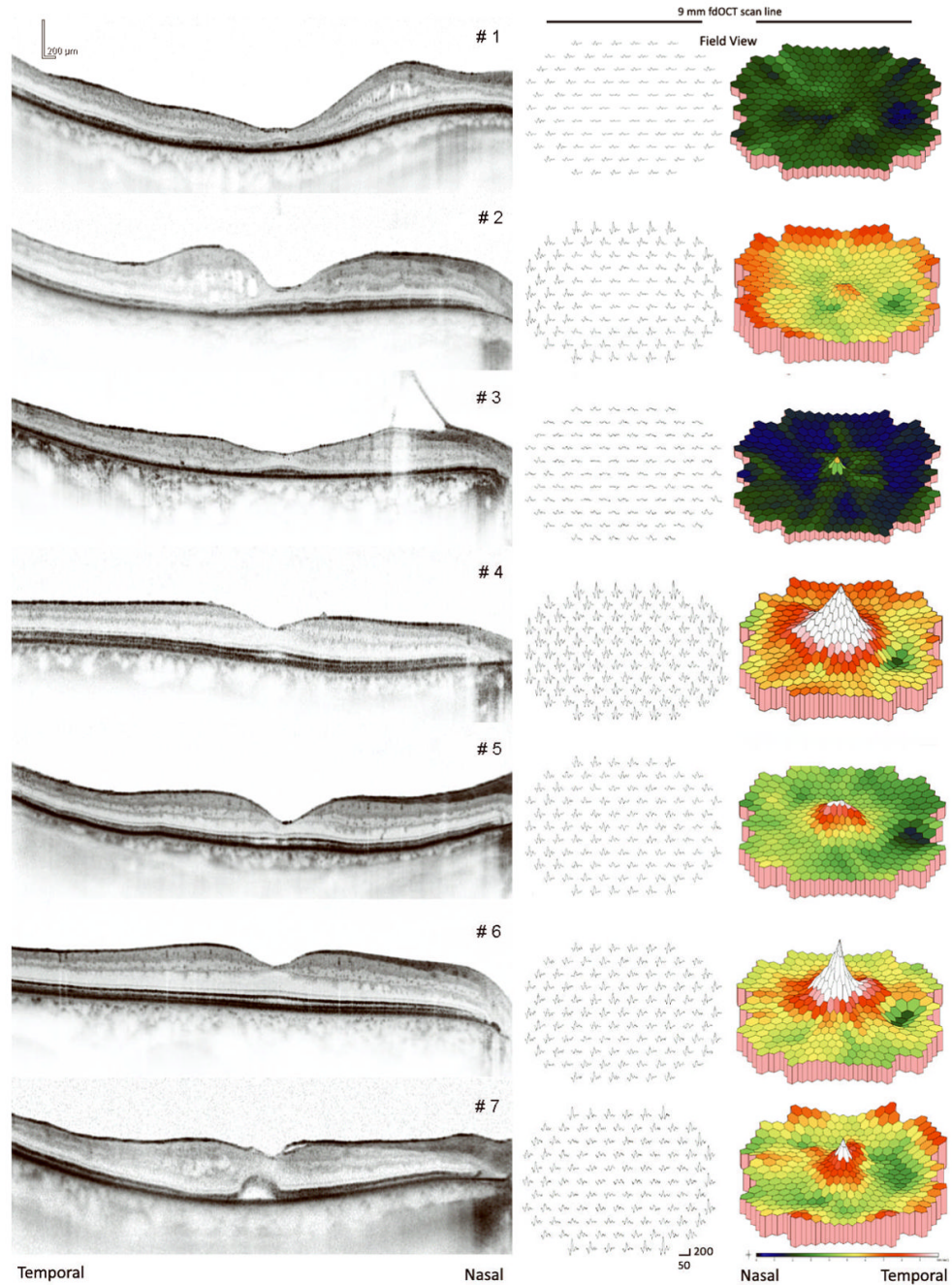
Figure 2.
Horizontal midline fdOCT scans and mfERG results from the right eyes of all seven patients. Left column: fdOCT scans from each patient; Middle column: mfERG responses shown in field view with calibration markers indicating 200 nV/deg^2 and 50 msec; Right column: mfERG density plots refined through interpolation with twice the resolution as the 103 stimulus hexagons.
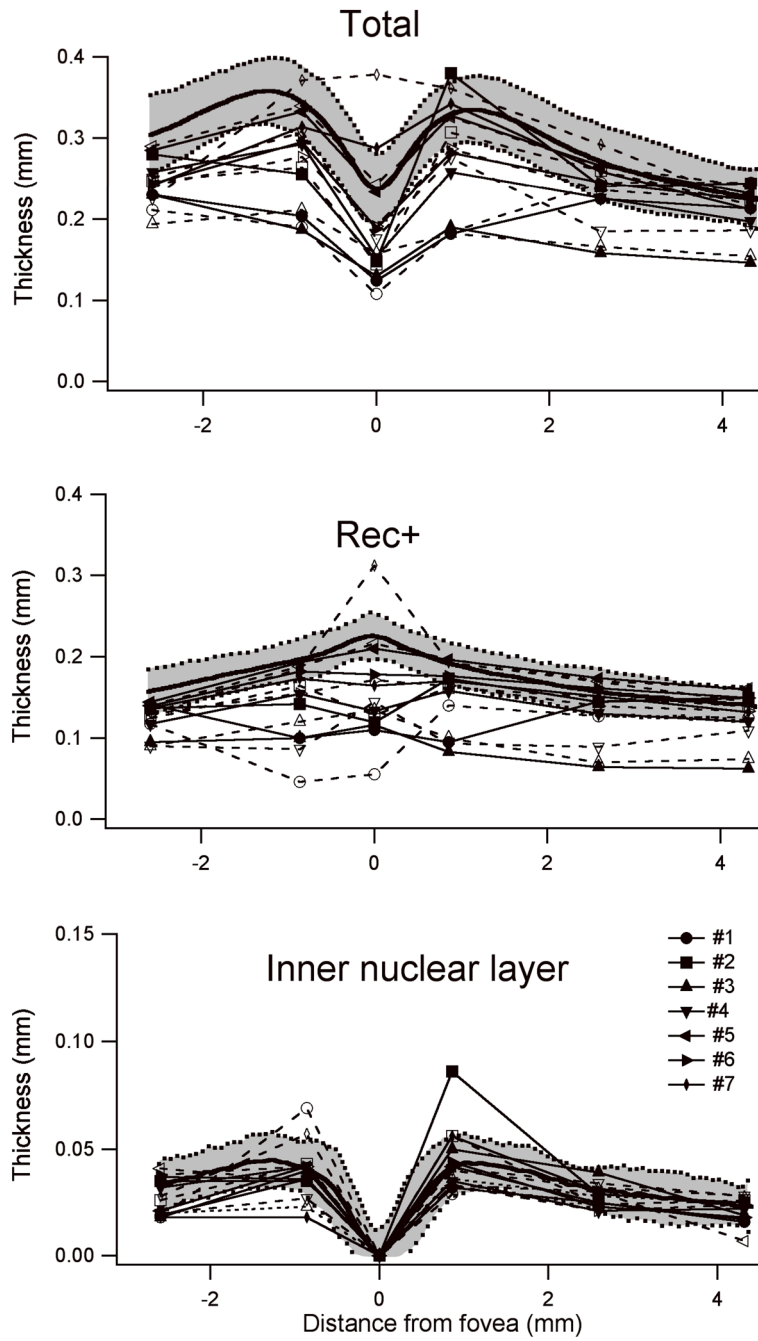
Figure 3.
Thickness measurements from fdOCTs. The solid curve is the mean of 23 normal subjects; the shaded area indicates ± 2 standard deviations. Closed symbols (solid lines) and open symbols (dashed lines) show OD and OS, respectively, of the same patient. Most patients show a reduction in total thickness throughout the macula. This is primarily due to a reduction in REC +. Inner nuclear layer thickness is normal except in two eyes with macular edema involving the inner retina.

Table 1

Demographic and clinical data

Patient	RFSW ID#	Age	Gender	Time with Diagnosis (yrs)	Treatments	Lens
1	7689	61	M	10	prednisone, azathioprine, acetazolamide, cyclosporine, triamcinolone, flucinolone implant (OS), 2nd glaucoma (OS)	IOL (OD) IOL (OS)
2	4764	57	F	13	flucinolone implant (OD), prednisone, acetazolamide, diclofenac drops, glaucoma tube (OD), 2nd glaucoma (OD)	IOL (OD) IOL (OS)
3	5026	72	F	13	diclofenac drops	+1 nuclear (OS) +2 nuclear (OD)
4	7986	54	M	6	cyclosporine, acyclovir, cellcept	+1 nuclear (OD) IOL (OS)
5	4771	80	M	13	prednisone, acetazolamide, cyclosporine, triamcinolone, flucinolone implant (OS), 2nd glaucoma (OS)	clear (OD) clear (OS)
6	7758	47	M	2	mycophenolate, triamcinolone, flucinolone implant (OD)	clear (OD) clear (OS)
7	3789	59	M	16	prednisone, diamox	clear (OD) clear (OS)

Table 2

Snellen visual acuity and OCT-3 data

Patient#	Eye	Snellen Acuity	OCT Foveal Thickness (μM)	OCT Macular Volume (mm^3)	Thin?	Macular Edema?
1	OD	20/200	117	5.346	Y	Y
	OS	20/200	139	5.965	Y	Y
2	OD	20/50	128	5.302	Y	Y
	OS	20/40	188	8.270	N	Y
3	OD	20/50	140	4.919	Y	N
	OS	20/50	133	5.027	Y	N
4	OD	20/20	171	5.46	N	N
	OS	20/25	163	5.71	N	N
5	OD	20/30	253	6.39	N	N
	OS	20/200	152	5.32	Y	N
6	OD	20/30	203	6.510	N	N
	OS	20/25	213	6.290	N	N
7	OD	20/25	248	6.93	N	Y
	OS	20/30	333	7.28	N	Y

Table 3

ETDRS visual acuity and electroretinography results

Pt #	Eye	VA logMAR	OCT Thin?	mfERG foveal nV/deg^2	mfERG ring 2 nV/deg^2	mfERG ring 3 nV/deg^2	mfERG ring 4 nV/deg^2	mfERG ring 5 nV/deg^2	mfERG ring 6 nV/deg^2	Mean mfERG nV/deg^2
		Mean normal value		105.7	61.6	41.9	33.4	27.4	28.6	49.8
1	**OD**	**1**	**Y**	**14.1**	**10.9**	**11.3**	**10.3**	**10.2**	**12.3**	**11.1**
1	**OS**	**1**	**Y**	**10.5**	**10.4**	**10.7**	**10.1**	**9.9**	**10.1**	**10.4**
2	**OD**	**0.4**	**Y**	**26.7**	**23.7**	**23.7**	**24.4**	**23.8**	**28.9**	**25.2**
2	OS	0.3	N	20.7	19.1	20.6	18.0	16.4	18.7	18.9
3	**OD**	**0.4**	**Y**	**10.0**	**8.1**	**6.3**	**5.8**	**6.4**	**9.4**	**7.7**
3	**OS**	**0.4**	**Y**	**25.9**	**17.5**	**15.7**	**16.3**	**15.3**	**13.8**	**17.4**
4	OD	0	N	102.9	72.8	55.8	40.2	33.8	37.6	57.1
4	OS	0.1	N	89.9	48.6	36.3	29.4	21.3	21.6	41.2
5	OD	0.2	N	33.1	29.6	23.6	18.6	14.3	15.9	22.5
5	**OS**	**1.0**	**Y**	**5.2**	**13.5**	**12.5**	**9.5**	**10.0**	**12.1**	**10.5**
6	OD	0.2	N	92.3	58.0	36.6	29.2	22.0	22.8	43.5
6	OS	0.1	N	54.7	31.1	23.4	18.0	13.4	12.1	25.5
7	OD	0.1	N	50.1	30.0	28.6	20.1	19.4	24.7	28.8
7	OS	0.2	N	31.4	27.7	20.1	15.3	14.5	20.9	21.7

Table 4

Snellen acuity, OCT-3, and mfERG results for patients with and without anatomic thinning

	Eyes With Anatomic Thinning n = 6	Eyes Without Anatomic Thinning n = 8	p
Mean Snellen acuity (logMAR)	0.7 ± 0.33	0.15 ± 0.09	0.0006
Mean foveal thickness (μM)	134.8 ± 11.9	221.5 ± 55.6	0.003
Mean macular volume (mm^3)	5.3 ± 0.39	6.6 ± 0.9	0.006
Mean foveal ERG (nV/deg^2)	15.4 ± 8.9	59.4 ± 31.6	0.006
Mean mfERG (nV/deg^2)	13.7 ± 6.5	32.4 ± 13.4	0.009